frontiers | Frontiers in Nuclear Engineering

TYPE Original Research
PUBLISHED 06 January 2023
DOI 10.3389/fnuen.2022.1082324

OPEN ACCESS

EDITED BY
Lelio Luzzi,
Politecnico di Milano, Italy

REVIEWED BY
Lionel Desgranges,
Commissariat à l'Energie Atomique et aux Energies Alternatives (CEA), France
Jacques Lechelle,
Commissariat à l'Energie Atomique et aux Energies Alternatives (CEA), France

*CORRESPONDENCE
Masashi Watanabe,
watanabe.masashi81@jaea.go.jp

SPECIALTY SECTION
This article was submitted to Nuclear Materials, a section of the journal Frontiers in Nuclear Engineering

RECEIVED 28 October 2022
ACCEPTED 13 December 2022
PUBLISHED 06 January 2023

CITATION
Watanabe M and Kato M (2023), Oxygen potential, oxygen diffusion, and defect equilibria in $UO_{2\pm x}$. *Front. Nucl. Eng.* 1:1082324. doi: 10.3389/fnuen.2022.1082324

Oxygen potential, oxygen diffusion, and defect equilibria in $UO_{2\pm x}$

Masashi Watanabe* and Masato Kato

Fuel Cycle Design Office, Japan Atomic Energy Agency, Oarai-machi, Japan

Since the oxygen potential and the oxygen diffusion coefficient of UO_2 have a significant impact on fuel performance, many experimental data have been obtained. However, experimental data of the oxygen potential and the oxygen diffusion coefficient in the high temperature region above 1673 K are very limited. In the present study, we aimed to obtain these data and analyze them by defect chemistry. the oxygen potentials and the oxygen chemical diffusion coefficient of UO2 were measured by the gas equilibrium method in the near stoichiometric region at temperatures ranging from 1673 to 1873 K. A data set of oxygen potentials was made together with literature data and analyzed by defect chemistry. The oxygen potential of UO_2 was determined as a function of O/U ratio and temperature, and an equation representing the relationship was derived. The oxygen chemical diffusion coefficient values obtained in this study were reasonably close to the literature values. The oxygen partial pressure dependence of the oxygen chemical diffusion coefficients was predicted from the evaluated results of the oxygen potential data, but no clear dependence was observed.

KEYWORDS

oxygen potential, oxygen chemical diffusion, defect chemistry, uranium dioxide, oxygen self-diffusion

1 Introduction

It is well-known that UO_2, which has a fluorite structure, is a non-stoichiometric oxide that is stable in the hyper-stoichiometric composition range. It has also been shown that UO_2 can lose oxygen to form a hypo-stoichiometric phase at high temperatures and low oxygen potentials. Many researchers have investigated oxygen potentials to determine the oxygen-to-uranium (O/U) ratio and chemical stability (Aronson and Belle 1958; Markin TL. and Bones RJ. 1962; Aukrust, Forland, and Hagemark 1962; Markin TL. and Bones RJ. 1962; Aitken, Brassfield, and Fryxell 1966; Hagemark and Broli 1966; Markin, Wheeler, and Bones 1968; Tetenbaum and Hunt 1968; Ackermann, Rauh, and Chandrasekharaiah 1969; Wheeler 1971; Javed 1972; Wheeler and Jones 1972; Chilton and Edwards 1980; Ugajin 1983), because its stoichiometry significantly affects thermal properties and fuel performance. Ugajin (1983) investigated the near-stoichiometric region by thermogravimetry in a mixed-gas atmosphere of CO/CO_2. Oxygen partial pressure was determined in situ with a stabilized zirconia oxygen sensor. Aronson and Belle (1958) and Markin and Bones (1962) determined the oxygen potential for O/U ratios in the range of 2.01 to 2.53 by the electromotive force (EMF) method. The oxygen potential in UO_{2-x} was also measured at temperatures above 1873 K using H_2 and CO gases (Wheeler 1971; Javed 1972), and various methods were employed in the measurements. However, the data were scattered over a range larger than 200 kJ/mol, especially when located in the near-stoichiometric region because of difficulty in determining the O/U ratio and oxygen potential pressure. The relationship between the O/U ratio, the temperature, and the oxygen potential has been represented in previous works. Lindemer and Besmann (1985) derived the relationship from the literature data and

TABLE 1 Impurities in the UO_2 raw powder.

Element	Concentration (ppm)
Ag	<0.2
Al	<10
B	<0.3
Bi	<5
Ca	<10
Cd	<0.6
Cr	<10
Cu	<1
Fe	10
Mg	<2
Mn	<6
Mo	<10
Ni	<10
Pb	<10
Si	<10
Sn	<10
Ti	<10
V	<10
Zn	<50

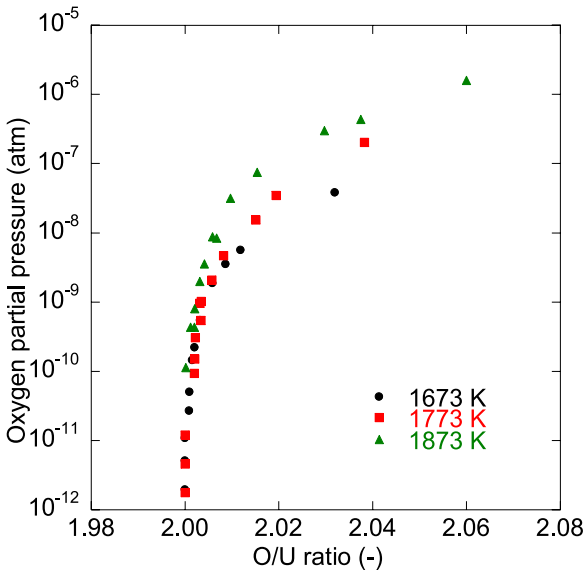

FIGURE 1
Oxygen potential measurement results at 1673 K, 1773 K, and 1873 K.

the classical thermodynamic theory for a solid solution. Some studies represented the relationship by means of the thermodynamic database (Guéneau et al., 2002; Baichi et al., 2006).

The diffusion kinetics for the oxygen ions in oxide fuels are closely involved in diffusion-controlled phenomena such as oxidation and reduction, sintering, and irradiation behavior. For this reason, the oxygen diffusion coefficients of UO_2 have been measured since the 1960s (Auskern and Belle 1961; Belle 1969; Bittel, Sjodahl, and White 1969; Marin and Contamin 1969; Lay 1970; Murch, Bradhurst, and De Bruin 1975; Breitung 1978; Murch and Thorn 1978; Kim and Olander 1981; Bayoglu and Lorenzelli 1984; Ruello et al., 2004). The oxidation and reduction of oxide fuels rely on chemical diffusion in thermodynamically non-ideal systems where oxygen ions are the faster species. The oxygen chemical diffusion coefficient, $\tilde{D}$, is generally obtained by measuring weight changes or electrical conductivity changes during redox reactions (Bittel, Sjodahl, and White 1969; Lay 1970; Bayoglu and Lorenzelli 1984; Ruello et al., 2004) and has been measured over a wide temperature range; but there are very few reports above 1673 K.

In this work, the oxygen potentials of UO_2 were obtained in hyper-stoichiometric compositions by the gas equilibrium method, a Brouwer diagram was constructed, and correlations to represent the O/U ratio were derived as functions of temperature and oxygen partial pressure. In addition, the oxygen chemical diffusion coefficients of UO_{2+x} in the temperature range above 1673 K were measured and compared with literature data, and the dependence of oxygen chemical diffusion coefficients on oxygen partial pressure was discussed.

2 Experimental procedures

Samples of UO_2 were prepared by powder metallurgy, with UO_2 powder made by the ammonium diuranate (ADU) process used as the starting material. The main impurities contained in the raw powder are listed in Table 1. The powder was pressed into a disk-like sample and sintered at 1973 K for 2.5 h in a gas mixture of 4.5% H_2–Ar, with added moisture. The amount of moisture was adjusted by passing 4.5% H_2–Ar mixed gas through a water bath kept at a constant temperature. The sample weight was 331.91 mg, and the size was 4.253 mm in diameter by 2.275 mm in thickness.

The oxygen potential and the oxygen chemical diffusion coefficient measurements were carried out at 1673 K, 1773 K, and 1873 K by the gas equilibrium method using a thermogravimeter (TG-DTA 2000SA, Bruker AXS). The uncertainty of the thermogravimeter was ±0.01 mg, which corresponds to ±0.0005 in the O/U ratio. In the measurements, it was observed that the sample weight was reduced by 60 μg/h. It was concluded that the high vapor pressure of the UO_3 species caused the large weight reduction. Due to the small sample volume and short time to reach equilibrium, the measurement of a data point was carried out in less than 30 min; therefore, the uncertainty in the O/U ratio determination was estimated to be ±0.00015.

The oxygen partial pressure in the atmosphere was controlled by the equilibrium reaction of $H_2O = H_2 + 1/2O_2$ and determined by oxygen sensors that measured the oxygen partial pressure at the equipment inlet and outlet. The gas phase equilibrium was related to the standard Gibbs free energy of formation of water, ΔG_f (J/mol), by the following equations (Kubaschewski and Alcock 1979)

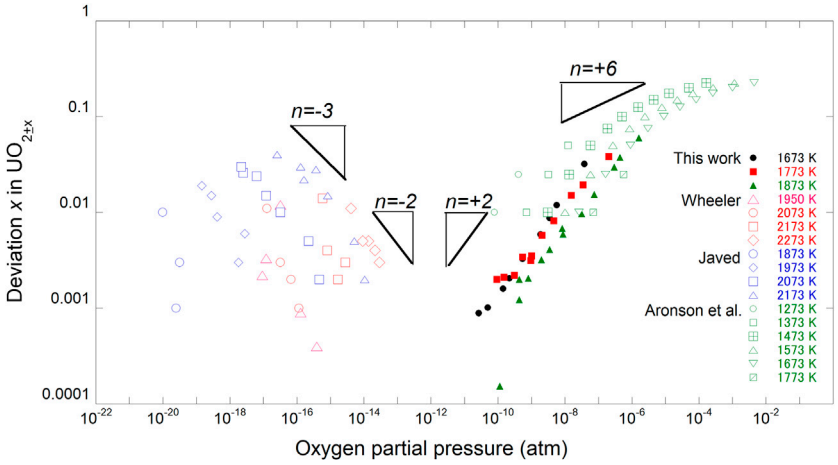

FIGURE 2
Relationships among oxygen partial pressures and deviations, x, in $UO_{2\pm x}$.

$$\Delta G_f = RT \ln \frac{P_{H_2O}}{P_{H_2} P_{O_2}^{1/2}}, \quad (1)$$

$$\Delta G_f = -246440 + 54.8T. \quad (2)$$

where R is the gas constant (8.3145 J/K/mol) and T is absolute temperature. Eq. 1 represents the value from 298 K to 2500 K. The ratio of P_{H_2O}/P_{H_2} was calculated using P_{O_2}, which was monitored at 973 K using an oxygen sensor. The P_{O_2} of the atmosphere in the thermogravimeter at higher temperature was calculated under the assumption that the P_{H_2O}/P_{H_2} ratio had the same value at the oxygen sensor and the thermogravimeter. The $\Delta\bar{G}_{O_2}$ was described by the following equation

$$\Delta\bar{G}_{O_2} = RT \ln P_{O_2}. \quad (3)$$

The uncertainty of $\Delta\bar{G}_{O_2}$ was estimated to be ±10 kJ/mol from the difference of P_{O_2} between the inlet and outlet gas. In the measurements, the change in specimen weight was measured in response to changes in P_{O_2} which were controlled by the ratio of P_{H_2O}/P_{H_2}. Equilibrium conditions were obtained in a relatively short time (~15 min) because of the smallness and thinness of the specimen disk. An effect of vaporization of the specimen on measurement data was not observed.

3 Results

The oxygen potential was measured at temperatures of 1673 K, 1773 K, and 1873 K, and data are shown in Figure 1. The P_{O_2} slightly increased with temperature, depending on the O/U ratio. The relationship between P_{O_2} and x is plotted in Figure 2. In this figure, the well-known proportionality relationship between P_{O_2} and deviation x from stoichiometry was observed:

$$x \propto P_{O_2}^{1/n}, \quad (4)$$

where n is a characteristic number identifying the type of point defect in agreement with literature data (Aronson and Belle 1958; Wheeler 1971; Javed 1972; Wheeler and Jones 1972). The figure shows that the present data changed in accordance with the relationship of $n = +2$. The literature data were also plotted in the figure and analyzed using the relationship of Eq. 4. In the higher P_{O_2} region, the relationship was $n = +6$. In the hypo-stoichiometric region, it was observed to be $n = -3$, as previously reported (Tetenbaum and Hunt 1968; Javed 1972).

TABLE 2 Experimental conditions, oxygen chemical diffusion coefficient $\tilde{D}$, and surface reaction rate constant, k.

No.	Temperature °K	O/U ratio		$\tilde{D}$	k
		Initial	Final	(m^2/s)	(m/s)
1	1673	2.116	2.082	3.73×10^{-8}	9.52×10^{-7}
2	1673	2.082	2.062	1.05×10^{-9}	2.77×10^{-6}
3	1673	2.074	2.037	3.47×10^{-8}	2.99×10^{-6}
4	1673	2.020	2.004	8.36×10^{-9}	1.03×10^{-5}
5	1773	2.115	2.070	8.66×10^{-8}	2.39×10^{-6}
6	1873	2.133	2.101	1.16×10^{-8}	1.57×10^{-6}
7	1873	2.101	2.080	2.38×10^{-7}	2.45×10^{-6}
8	1873	2.068	2.050	6.24×10^{-8}	3.87×10^{-7}
9	1873	2.050	2.028	1.20×10^{-8}	7.45×10^{-6}

Since the specimen used in this work had the shape of a planar sheet, the diffusion equation was set up for planar sheet geometry with a thickness of 2L. If the sheet is initially at a uniform concentration, C_1, and the surface condition (Crank 1979) is such that

$$-D\frac{\partial C}{\partial x}\Big|_{x=\pm l} = k(C_0 - C_s), \quad (5)$$

where D is the diffusion coefficient, C is the concentration of diffusing substance in the planar sheet, k is the rate constant for surface reaction, C_s is the actual concentration just within the planar sheet, and C_0 is the concentration required to maintain equilibrium with the surrounding atmosphere. The obtained solution is

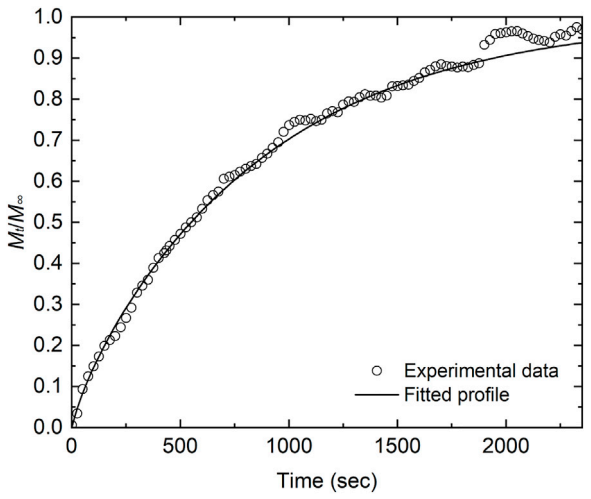

FIGURE 3
Experimental data and fitted curves after variation of the O/U ratio from 2.082 to 2.062 at 1673 K. The experimental data correspond to No. 2 in Table 2.

$$\frac{C-C_1}{C_0-C_1}=1-\sum_{n=1}^{\infty}\frac{2L\cos\left(\beta_n x/l\right)\exp\left(-\beta_n^2 Dt/l^2\right)}{\left(\beta_n^2+L^2+L\right)\cos\beta_n}, \tag{6}$$

where the β_n values are the positive roots of

$$\beta\tan\beta=L. \tag{7}$$

and

$$L=lk/D. \tag{8}$$

is a dimensionless parameter. The total amount of diffusing substance, M_t, entering or leaving the sheet up to time t is expressed as a fraction of M_∞, the corresponding quantity after infinite time, by

$$\frac{M_t}{M_\infty}=1-\sum_{n=1}^{\infty}\frac{2L^2\exp\left(-\beta_n^2 Dt/l^2\right)}{\beta_n^2\left(\beta_n^2+L^2+L\right)}. \tag{9}$$

The measured data were fitted by Eq. 9 using D and k as parameters. The experimental conditions and the fitting results are listed in Table 2, and Figure 3 shows the weight-change curve and the fitted curve at 1673 K. Good agreement can be seen between the experimental data and the fitted curve. The error in the oxygen chemical diffusion coefficient was calculated to be 84%. It is presumed that the periodic noise from the thermogravimeter degraded the fitting accuracy.

4 Discussion

The relationships among n = +6, +2, and −3 are shown in Figure 2. Two types of Brouwer diagram are proposed depending on the kinds of dominant point defects: intrinsic defects and Frenkel defects. The reported electrical conductivity measurements showed that the electronic conduction mechanism was observed, therefore, it is assumed that intrinsic defects were dominant in the stoichiometric composition. Cooper et al. (2018) calculated a Brouwer diagram of UO_2 using an *ab initio* approach in which intrinsic defects were dominant. In the near stoichiometric region, defect equilibria were considered in reactions (10)–(13):

$$O_O^{\times}\rightarrow V_O^{\cdot\cdot}+2e'+\frac{1}{2}O_2. \tag{10}$$

$$\frac{1}{2}O_2\rightarrow O_i''+2h^{\cdot}. \tag{11}$$

$$\text{null}\rightarrow e'+h^{\cdot}. \tag{12}$$

$$O_O^{\times}\rightarrow V_O^{\cdot\cdot}+O_i''. \tag{13}$$

The equilibrium constants in the aforementioned defect reactions can be described by Eqs 14–17, respectively:

$$K_V=\left[V_O^{\cdot\cdot}\right]\left[e'\right]^2P_{O_2}^{1/2}, \tag{14}$$

$$K_O=\left[O_i''\right]\left[h^{\cdot}\right]^2P_{O_2}^{-1/2}, \tag{15}$$

$$K_i=\left[e'\right]\left[h^{\cdot}\right], \tag{16}$$

$$K_F=\left[V_O^{\cdot\cdot}\right]\left[O_i''\right]. \tag{17}$$

In the case where intrinsic defects are dominant, the defect concentrations of e' and $h^{\cdot}$ dominate over those of $V_O^{\cdot\cdot}$ and O_i''. Therefore, $[e']=[h^{\cdot}]$ near the stoichiometric region. The following Eqs 18–20 were obtained from 14–17:

$$\left[e'\right]=\left[h^{\cdot}\right]=K_i^{1/2}, \tag{18}$$

$$\left[O_i''\right]=\left(\frac{K_O}{K_i}\right)\cdot P_{O_2}^{1/2}=K_{n=+2}\cdot P_{O_2}^{1/2}, \tag{19}$$

$$\left[V_O^{\cdot\cdot}\right]=\left(\frac{K_V}{K_i}\right)\cdot P_{O_2}^{-1/2}=K_{n=-2}\cdot P_{O_2}^{-1/2}. \tag{20}$$

K_F was obtained from experimental and literature data in the near-stoichiometric region as follows:

$$K_F=K_{n=-2}\cdot K_{n=+2}=\frac{K_VK_O}{K_i^2}. \tag{21}$$

In the oxidation region where n = +2, the (2:2:2) Willis cluster (Willis 1987) was assumed as follows:

$$2O_O^{\times}+O_2\rightarrow\left(2O_i^{a}2O_i^{b}2V_O\right)'+h^{\cdot}\ \text{for}\ n=+2. \tag{22}$$

The equilibrium constant in the aforementioned defect reaction can be described by the following equation:

$$K_{ox}=\left[\left(2O_i^{a}2O_i^{b}2V_O\right)'\right]\left[h^{\cdot}\right]P_{O_2}^{-1}. \tag{23}$$

$[O_i'']$ can be written as

$$\left[O_i''\right]=2\left[\left(2O_i^{a}2O_i^{b}2V_O\right)'\right]=2K_{ox}^{1/2}P_{O_2}^{1/2}. \tag{24}$$

In the hypo-stoichiometric region, n = −3 has been reported by previous studies (Tetenbaum and Hunt 1968; Javed 1972). Kofstad proposed that interstitial uranium ions with two effective charges, $M_i^{\cdot\cdot}$, predominated in this region (Kofstad 1972). The following reaction was assumed:

$$2O_O^{\times}+M_M^{\times}\rightarrow M_i^{\cdot\cdot}+2e'+O_2\ \text{for}\ n=-3, \tag{25}$$

$$\left[M_i^{\cdot\cdot}\right]=\frac{1}{2}\left(2K_{n=-3}\right)^{1/3}P_{O_2}^{-1/3}. \tag{26}$$

In the oxidation region where n = +6, more complex defects were expected; however, there have been no reports describing this relationship. Defect reactions were not assumed in this region, and

TABLE 3 Defect formation energies of UO_2 and PuO_2.

	UO_2		PuO_2 (Kato et al., 2017)	
	ΔH (kJ/mol)	ΔS (J/mol/K)	ΔH (kJ/mol)	ΔS (J/mol/K)
$K_{n=+6}$	-130	-81.0	-	-
K_{ox}	-173.0	-38.1	-	-
$K_{n=+2}$	-60.0	5.0	159.3	-4.66
$K_{n=-2}$	464.5	32.0	282.5	54.66
$K_{n=-3}$	1,079.1	95.0	-	-
K_i	300.0	85.1	325	85
K_F	404.5	37.0	441.8	50
K_O	240.0	90.1	484.3	80.34
K_v	764.5	117.1	607.5	134.7

only the relationship of n = +6 was described by the following equation:

$$\left[\mathrm{O}_\mathrm{i}^{''}\right] = K_{n=+6}P_{O_2}^{1/6}. \tag{27}$$

The relationships of n = +2 and −2 should be observed in the near-stoichiometric region because intrinsic ionization dominates. The relationships among n = −3, +2 and +6, are shown in Figure 2. The experimental data were fitted by Eqs. 26 and 19–27 assuming that $x = [\mathrm{M}_\mathrm{i}^{\cdot\cdot\cdot\cdot}]$, $[\mathrm{V}^{\cdot\cdot}]$, or $[\mathrm{O}^{''}]$, and the equilibrium constants were obtained for each temperature. The equilibrium constant, K, in the defect reactions can be written as

$$K = \exp\left(\frac{\Delta S}{R}\right)\exp\left(-\frac{\Delta H}{RT}\right). \tag{28}$$

Enthalpy, ΔH (J/mol), and entropy, ΔS (J/mol/K), for the equilibrium constants were evaluated as follows:

$$K_{n=-3} = \exp\left(\frac{95.0}{R}\right)\exp\left(-\frac{1079.1\times10^3}{RT}\right). \tag{29}$$

$$K_{ox} = \exp\left(\frac{-38.1}{R}\right)\exp\left(\frac{173.0\times10^3}{RT}\right). \tag{30}$$

$$K_{n=+6} = \exp\left(\frac{-81.0}{R}\right)\exp\left(\frac{130.0\times10^3}{RT}\right). \tag{31}$$

In addition, it was assumed that Eq. 19 equals Eq. 24. The ΔH and ΔS in each region are shown in Table 3. Eqs 17–27 describe the Brouwer diagram as shown in Figure 4. The figure shows that the Brouwer diagrams at 1673, 1773, and 1873 K represented the experimental data very well. The Brouwer diagram can give the defect concentrations of $[\mathrm{V}_\mathrm{O}^{\cdot\cdot}]$ and $[\mathrm{O}_\mathrm{i}^{''}]$. The O/U ratio can be described as Eq. 32, when the main defects are $[\mathrm{V}_\mathrm{O}^{\cdot\cdot}]$ or $[\mathrm{O}_\mathrm{i}^{''}]$:

$$\frac{\mathrm{O}}{\mathrm{U}}\ \text{ratio} = 2 - \left[\mathrm{V}_\mathrm{O}^{\cdot\cdot}\right] + \left[\mathrm{O}_\mathrm{i}^{''}\right]. \tag{32}$$

$[\mathrm{V}_\mathrm{O}^{\cdot\cdot}]$ and $[\mathrm{O}_\mathrm{i}^{''}]$ can be described in Eqs. 33 and 34 using Eqs. 19–27, respectively. The indices −5 and −1/5 are parameters that represent x near the boundary between each line:

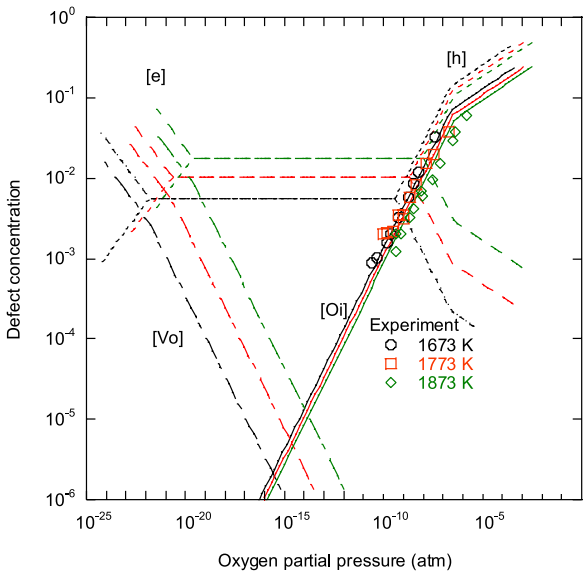

FIGURE 4
Brouwer diagram of $UO_{2\pm x}$ at 1673 K, 1773 K, and 1873 K.

$$\left[\mathrm{V}_\mathrm{O}^{\cdot\cdot}\right] = \left\{\left(K_{n=-2}P_{O_2}^{-1/2}\right)^{-5} + \left((2K_{n=-3})^{1/3}P_{O_2}^{-1/3}\right)^{-5}\right\}^{-1/5}, \tag{33}$$

$$\left[\mathrm{O}_\mathrm{i}^{''}\right] = \left\{\left(K_{n=+2}P_{O_2}^{1/2}\right)^{-5} + \left((K_{n=6})^{1/3}P_{O_2}^{-1/6}\right)^{-5}\right\}^{-1/5}. \tag{34}$$

Eq. 32 was rewritten as Eq. 35 using Eqs 33 and 34, which can represent the O/U ratio as functions of P_{O_2} and T:

$$\begin{aligned}\frac{\mathrm{O}}{\mathrm{U}}\ \text{ratio} = 2 - &\left\{\left(\exp\left(\frac{32.0}{R}\right)\exp\left(-\frac{464500}{RT}\right)P_{O_2}^{-1/2}\right)^{-5}\right.\\ &\left.+\left(\left(2\exp\left(\frac{95.0}{R}\right)\exp\left(-\frac{1079100}{RT}\right)\right)^{1/3}P_{O_2}^{-1/3}\right)^{-5}\right\}^{-1/5}\\ &+\left\{\left(\exp\left(\frac{5.0}{R}\right)\exp\left(\frac{60000}{RT}\right)P_{O_2}^{1/2}\right)^{-5}\right.\\ &\left.+\left(\left(\left(\exp\left(\frac{-81.0}{R}\right)\exp\left(\frac{130000}{RT}\right)\right)^{1/3}\right)P_{O_2}^{1/6}\right)^{-5}\right\}^{-1/5}.\end{aligned} \tag{35}$$

Eq. 35 gives the relationships between oxygen potential, temperature, and composition in $UO_{2\pm x}$. Figure 5 shows the relationships between x, T, and P_{O_2} and literature data (Aronson and Belle 1958; Wheeler 1971; Javed 1972; Wheeler and Jones 1972).

The ΔH and ΔS for the equilibrium constants were assessed as shown in Table 3. The formation energies of $\mathrm{O}_\mathrm{i}^{''}$, $\mathrm{V}_\mathrm{O}^{\cdot\cdot}$, $(\mathrm{V}_\mathrm{O}^{\cdot\cdot} + \mathrm{O}_\mathrm{i}^{''})$, and $(\mathrm{e}' + \mathrm{h}^{\cdot})$ in UO_2 were -60.0 kJ/mol, 464.5 kJ/mol, 404.5 kJ/mol, and 300.0 kJ/mol, respectively. The Frenkel defect formation energy was compared with literature data (Catlow and Lidiard 1974; Catlow 1977; Clausen et al., 1984; Jackson et al., 1986; Matzke 1987; Murch and Catlow 1987; Petit et al., 1998; Crocombette et al., 2001; Freyss, Petit, and Crocombette 2005; Iwasawa et al., 2006; Gupta, Brillant, and Pasturel 2007; Terentyev 2007; Yun and Kim 2007; Nerikar et al., 2009; Tiwary, van de Walle, and Gronbech-Jensen 2009; Yu, Devanathan, and Weber 2009; Staicu et al., 2010; Andersson et al., 2011; Freyss et al., 2012; Konings and Benes 2013; Vathonne et al., 2014), as shown

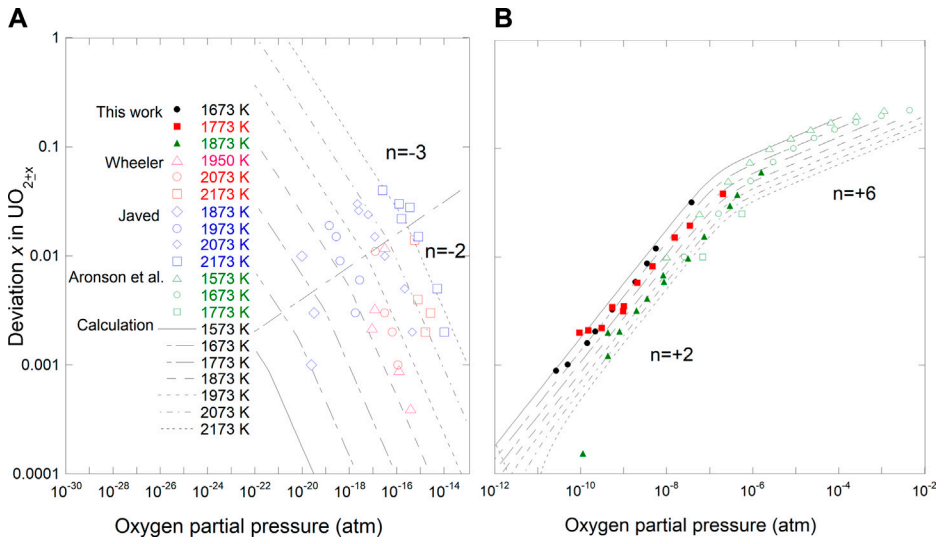

FIGURE 5
Comparison of deviation from stoichiometry vs temperature and oxygen partial pressure with calculated results using Eq. (35). **(A)** hypo-stoichiometric region; **(B)** hyper-stoichiometric region.

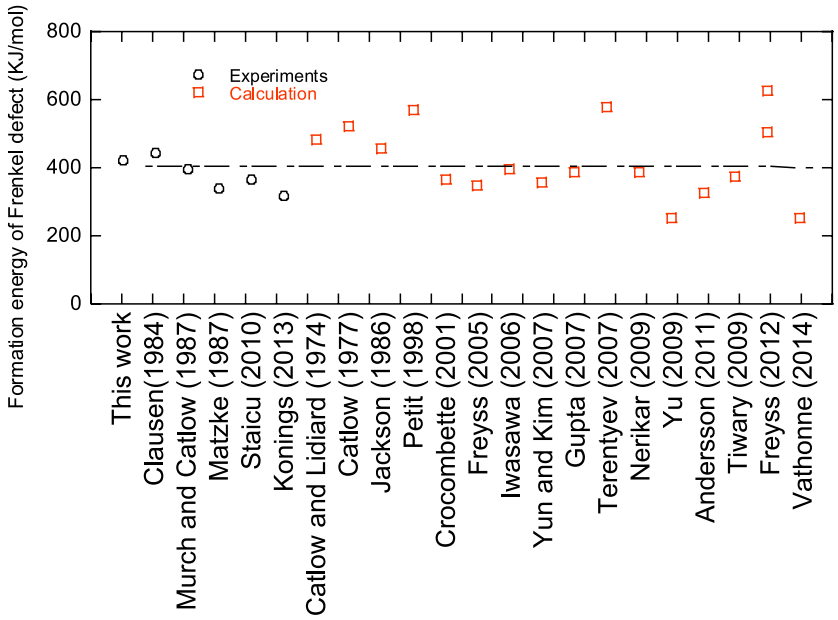

FIGURE 6
Comparison of Frenkel defect formation energy in $UO_{2\pm x}$.

in Figure 6. The present data approximately corresponded to literature data, which were obtained by experiments and calculations. The Frenkel defect formation energies of UO_2were compared with those of PuO_2 (Kato et al., 2017) and they are almost the same (Table 3). The formation energy value for O_i'' is lower in UO_2 than in PuO_2, -60.0 kJ/mol and 159.3 kJ/mol, respectively. Conversely, the formation energy value for $V_O^{\cdot\cdot}$ is lower in PuO_2 than in UO_2, 282.5 kJ/mol and 464.5 kJ/mol, respectively. These differences are caused by changing from M^{4+} to U^{5+} and Pu^{3+}, respectively, in UO_2 and PuO_2.

Figure 7 shows a comparison between the experimental data (Aronson and Belle 1958; Markin TL. and Bones RJ. 1962; Aukrust, Forland, and Hagemark 1962; Markin TL. and Bones RJ. 1962; Aitken, Brassfield, and Fryxell 1966; Hagemark and Broli 1966; Markin, Wheeler, and Bones 1968; Tetenbaum and Hunt 1968; Ackermann, Rauh, and Chandrasekharaiah 1969; Wheeler 1971; Javed 1972; Wheeler and Jones 1972; Chilton and Edwards 1980; Ugajin 1983) and the calculated results of the oxygen potential of UO_2. The results of the calculations represent the data within σ = ±51 kJ/mol. It can be seen that there is no large discrepancy

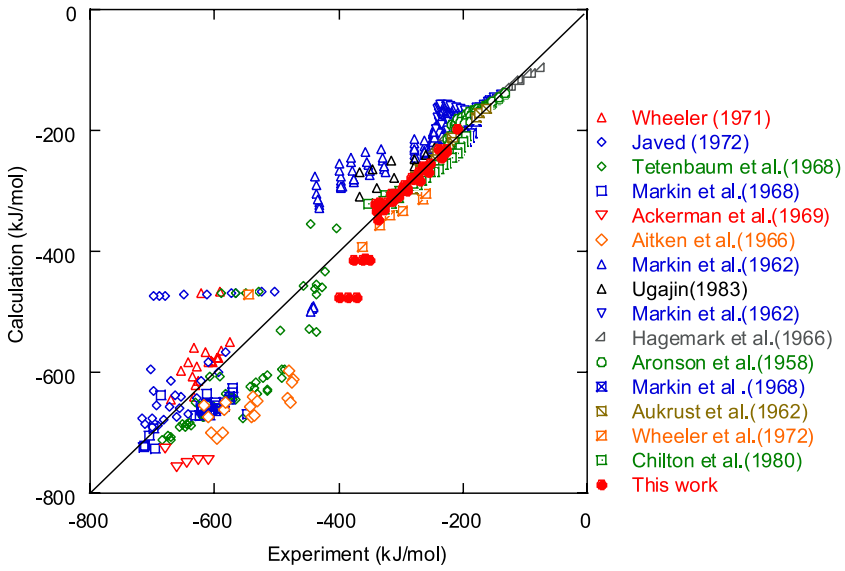

FIGURE 7
Comparison between measured and calculated data.

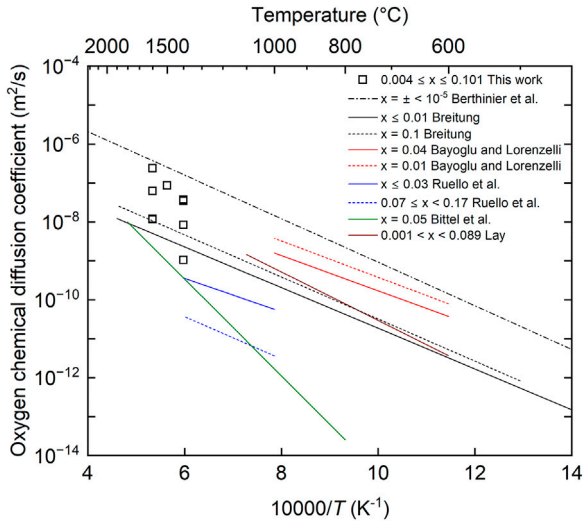

FIGURE 8
Comparison between oxygen chemical diffusion coefficients in this work and literature data.

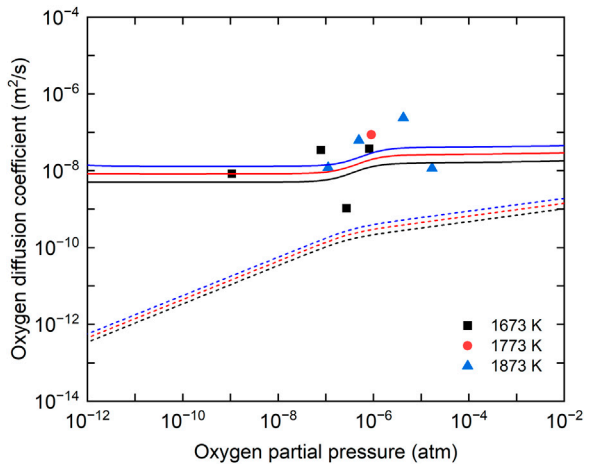

FIGURE 9
Dependence of measured oxygen chemical diffusion coefficients on oxygen partial pressure with calculation results. Solid lines show the calculation results of the oxygen chemical diffusion coefficients. Dashed lines show the calculation results of oxygen self-diffusion coefficients.

between the calculated values and the literature values in the hyper-stoichiometric composition range, but there is a large discrepancy in the near- and hypo-stoichiometric regions where there are few experimental data (Figure 7). Especially in the near-stoichiometric region, further expansion of experimental data is necessary, but it is greatly affected by impurities (Maillard et al., 2022); thus, it is necessary to reduce the impurities in the sample to obtain highly accurate data.

Figure 8 shows the comparison between the oxygen chemical diffusion coefficients measured in this study and the literature data (Bittel, Sjodahl, and White 1969; Lay 1970; Breitung 1978; Bayoglu and Lorenzelli 1979; Ruello et al., 2004; Berthinier et al., 2013). The data obtained in this study have larger values than those reported by Bittel et al. and Breitung, but smaller values than those in the near-stoichiometric composition proposed by Berthinier et al. (2013). The data reported by Bittel et al. are the only experimental data in the temperature range above 1673 K. They evaluated the oxygen chemical diffusion coefficients from the results of the steam oxidation of UO_2, but it was pointed out that the U_4O_9 phase was formed on the sample surface, which caused the evaluated oxygen chemical diffusion coefficients to be lower (Breitung 1978). According to the calculation results

reported by Berthinier et al., the oxygen chemical diffusion coefficients had maximum values near the stoichiometric composition and decreased with increasing deviation from the stoichiometric composition (Berthinier et al., 2013). Thus, the oxygen chemical diffusion coefficients measured in this study can be considered reasonable, in general. The dependence of the measured diffusion coefficients on oxygen partial pressure is shown in Figure 9. The oxygen chemical diffusion coefficients and the oxygen self-diffusion coefficients (D^*) are related by Darken's relationship as given by:

$$\tilde{D} = \frac{2 \pm x}{2x} D^* \left(\pm \frac{\partial \log P_{O_2}}{\partial \log x} \right), \tag{36}$$

where the positive and negative signs apply to the hyper- and hypo-stoichiometric ranges, respectively. The oxygen self-diffusion coefficient follows the equation of (Berthinier et al., 2013; Watanabe, Kato, and Sunaoshi 2020)

$$D^* = D^0_{V_O} \left[V^{\cdot\cdot}_O \right] \exp\left(-\frac{\Delta H^m_{V_O}}{RT} \right) + 2 D^0_{O_i} \left[O^{''}_i \right] \exp\left(-\frac{\Delta H^m_{O_i}}{RT} \right), \tag{37}$$

where $D^0_{V_O}$ is the pre-exponential term for the oxygen vacancy diffusion, $D^0_{O_i}$ is the pre-exponential term for oxygen interstitial diffusion, $\Delta H^m_{V_O}$ is the migration energy of the oxygen vacancy, and $\Delta H^m_{O_i}$ is the migration energy of the oxygen interstitial. The $[V^{\cdot\cdot}_O]$ and $[O^{''}_i]$ in Eq. 37 can be calculated by Eqs 33 and 34. The oxygen self-diffusion coefficient can be calculated by using the pre-exponential terms and the migration energies evaluated by Kato et al. The oxygen chemical diffusion coefficients can be derived from Eqs 36 and 37, and the calculation results are shown in Figure 9. Since the oxygen chemical diffusion coefficients were measured in the regions of $n = +2$ and $n = +6$, it is considered that the oxygen diffusion coefficients were dependent on the oxygen partial pressure; however, the oxygen partial pressure dependence was not clearly observed in this study.

5 Conclusions

The oxygen potentials and oxygen chemical diffusion coefficients of UO_2 were measured by the gas equilibrium method. A data set of oxygen potential was made and analyzed based on defect chemistry. The relationships between deviation x from stoichiometric composition and the oxygen partial pressure were investigated. Defect equilibrium constants were evaluated by fitting the experimental data and defect formation energies were determined and used to construct a Brouwer diagram. The correlation with UO_2 oxygen potential was then derived. The correlation described the oxygen potential very well even in the near-stoichiometric composition range. The oxygen Frenkel formation energy was estimated to be 404.5 kJ/mol, which was in good agreement with literature values. As a result of comparison with the literature values, it was found that the values of the oxygen chemical diffusion coefficients obtained in this study were generally reasonable. The oxygen partial pressure dependence of the oxygen chemical diffusion coefficient was predicted from the evaluated results of the oxygen potential data, but no clear dependence was observed.

Data availability statement

The original contributions presented in the study are included in the article/Supplementary Material, further inquiries can be directed to the corresponding author.

Author contributions

MW: investigation, analysis, and writing the original draft; MK: conceptualization, analysis, and reviewing and editing the original draft.

Conflict of interest

The authors declare that the research was conducted in the absence of any commercial or financial relationships that could be construed as a potential conflict of interest.

Publisher's note

References

Ackermann, R. J., Rauh, E. G., and Chandrasekharaiah, M. S. (1969). 'Thermodynamics study of the urania-uranium system. *J. Phys. Chem.* 73, 762–769. doi:10.1021/j100724a002

Aitken, E. A., Brassfield, H. C., and Fryxell, R. E. (1966). "Thermodynamic behaviour of hypostoichiometric UO_2," in *Conference: Symposium on thermodynamics with emphasis on nuclear materials and atomic transport in solids* (Vienna (Austria), 435–453.

Andersson, D. A., Uberuaga, B. P., Nerikar, P. V., Unal, C., and Stanek, C. R. (2011). U and Xe transport in UO2±x: Density functional theory calculations. *Phys. Rev. B* 84, 054105. doi:10.1103/physrevb.84.054105

Aronson, S., and Belle, J. (1958). 'Nonstoichiometry in uranium dioxide. *J. Chem. Phys.* 29, 151–158. doi:10.1063/1.1744415

Aukrust, E., Forland, T., and Hagemark, K. (1962). "Equilibrium measurements and interpretation of non-stoichiometry in UO_{2+x}," in *Thermodynamics of nuclear materials* (Vienna: IAEA), 713–722.

Auskern, A. B., and Belle, J. (1961). 'Oxygen ion self-diffusion in uranium dioxide. *J. Nucl. Mater.* 3, 267–276. doi:10.1016/0022-3115(61)90194-5

Baichi, M., Chatillon, C., Ducros, G., and Froment, K. (2006). 'Thermodynamics of the O–U system. IV – critical assessment of chemical potentials in the U–$UO_{2.01}$ composition range. *J. Nucl. Mater.* 349, 17–56. doi:10.1016/j.jnucmat.2005.09.001

Bayoglu, A., and Lorenzelli, R. (1984). 'Oxygen diffusion in fcc fluorite type nonstoichiometric nuclear oxides MO2±x☆', *Solid State Ionics*, 12, 53–66. doi:10.1016/0167-2738(84)90130-9

Bayoglu, A. S., and Lorenzelli, R. (1979). 'Etude de la diffusion chimique de l'oxygene dans puo2−x par dilatometrie et thermogravimetrie. *J. Nucl. Mater.* 82, 403–410. doi:10.1016/0022-3115(79)90022-9

Belle, J. (1969). 'Oxygen and uranium diffusion in uranium dioxide (a review). *J. Nucl. Mater.* 30, 3–15. doi:10.1016/0022-3115(69)90163-9

Berthinier, C., Rado, C., Chatillon, C., and Hodaj, F. (2013). 'Thermodynamic assessment of oxygen diffusion in non-stoichiometric UO2±x from experimental data and Frenkel pair modeling. *J. Nucl. Mater.* 433, 265–286. doi:10.1016/j.jnucmat.2012.09.011

Bittel, J. T., Sjodahl, L. H., and White, J. F. (1969). 'Steam oxidation kinetics and oxygen diffusion in UOz at high temperatures. *J. Am. Ceram. Soc.* 52, 446–451. doi:10.1111/j.1151-2916.1969.tb11976.x

Breitung, W. (1978). Oxygen self and chemical diffusion coefficients in. *J. Nucl. Mater.* 74, 10–18. doi:10.1016/0022-3115(78)90527-5

Catlow, C. R. A. (1977). 'Point-Defect and electronic properties of uranium-dioxide. *Proc. R. Soc. Lond. Ser. a-Mathematical Phys. Eng. Sci.* 353, 533–561.

Catlow, C. R. A., and Lidiard, A. B. (1974). Symposium on the thermodynamics of nuclear materials, 27-42. Vienna, Austria: IAEA.*Theoretical studies of point-defect properties of uranium dioxide.*

Chilton, G. R., and Edwards, J. (1980). Oxygen potentials of $U_{0.77}Pu_{0.23}O_{2+x}$ in the temperature range 1523-1822 K." 17, *United Kingdom Atomic Energy Authority, Northern Division*In.

Clausen, K., Hayes, W., Macdonald, J. E., Osborn, R., and Hutchings, M. T. (1984). 'Observation of oxygen Frenkel disorder in uranium-dioxide above 2000-K by use of neutron-scattering techniques. *Phys. Rev. Lett.* 52, 1238–1241. doi:10.1103/physrevlett.52.1238

Cooper, M. W. D., Murphy, S. T., and Andersson, D. A. (2018). 'The defect chemistry of $UO_{2\pm x}$ from atomistic simulations. *J. Nucl. Mater.* 504, 251–260. doi:10.1016/j.jnucmat.2018.02.034

Crank, J. (1979). *The mathematics of diffusion*. Oxford, United Kingdom, Oxford University Press.

Crocombette, J. P., Jollet, F., Nga, L. N., and Petit, T. (2001). 'Plane-wave pseudopotential study of point defects in uranium dioxide. *Phys. Rev. B* 64, 104107. doi:10.1103/physrevb.64.104107

Freyss, M., Dorado, B., Bertolus, M., Jomard, G., Vathonne, E., Garcia, P., et al. (2012). "First-principles DFT + U study of radiation damage in UO_2 : f electron correlations and the local energy minima issue," in *Psi-k newsletter*, 35–61.

Freyss, M., Petit, T., and Crocombette, J. P. (2005). 'Point defects in uranium dioxide: *Ab initio* pseudopotential approach in the generalized gradient approximation. *J. Nucl. Mater.* 347, 44–51. doi:10.1016/j.jnucmat.2005.07.003

Guéneau, C., Baichi, M., Labroche, D., Chatillon, C., and Sundman, B. (2002). 'Thermodynamic assessment of the uranium–oxygen system. *J. Nucl. Mater.* 304, 161–175. doi:10.1016/s0022-3115(02)00878-4

Gupta, F., Brillant, G., and Pasturel, A. (2007). 'Correlation effects and energetics of point defects in uranium dioxide: A first principle investigation. *Philos. Mag.* 87, 2561–2569. doi:10.1080/14786430701235814

Hagemark, K., and Broli, M. (1966). 'Equilibrium oxygen pressures over the nonstoicheiometric uranium oxides UO_{2+x} and U_3O_{8-z} at higher temperatures. *J. Inorg. Nucl. Chem.* 28, 2837–2850. doi:10.1016/0022-1902(66)80010-6

Iwasawa, M., Chen, Y., Kaneta, Y., Ohnuma, T., Geng, H. Y., and Kinoshita, M. (2006). 'First-principles calculation of point defects in uranium dioxide. *Mater. Trans.* 47, 2651–2657. doi:10.2320/matertrans.47.2651

Jackson, R. A., Murray, A. D., Harding, J. H., and Catlow, C. R. A. (1986). The calculation of defect parameters in UO_2. *Philosophical Mag. a-Physics Condens. Matter Struct. Defects Mech. Prop.* 53, 27–50. doi:10.1080/01418618608242805

Javed, N. A. (1972). 'Thermodynamic study of hypostoichiometric urania. *J. Nucl. Mater.* 43, 219–224. doi:10.1016/0022-3115(72)90053-0

Kato, M., Nakamura, H., Watanabe, M., Matsumoto, T., and Machida, M. (2017). Defect chemistry and basic properties of non-stoichiometric PuO_2. *Defect Diffusion Forum* 375, 57–70. doi:10.4028/www.scientific.net/ddf.375.57

Kato, M., Watanabe, M., Hirooka, S., and Vauchy, R. (In press 2023). Oxygen diffusion in flurotite-tyoe oxides, CeO_2, ThO_2, UO_2, PuO_2, and (U, Pu)O_2. *Front. Nucl. Eng.*

Kim, K. C., and Olander, D. R. (1981). Oxygen diffusion in UO2−x. *J. Nucl. Mater.* 102, 192–199. doi:10.1016/0022-3115(81)90559-6

Kofstad, P. (1972). *Nonstoichiometry, diffusion, and electrical conductivity in binary metal oxides*. Hoboken, New Jersey, United States, John Wiley & Sons.

Konings, R. J. M., and Benes, O. (2013). 'The heat capacity of NpO2 at high temperatures: The effect of oxygen Frenkel pair formation. *J. Phys. Chem. Solids* 74, 653–655. doi:10.1016/j.jpcs.2012.12.018

Kubaschewski, O., and Alcock, C. B. (1979). *Metallurgical thermochemistry*. Pergamon; 5th edition, Pergamon, Turkey.

Lay, K. W. (1970). 'Oxygen chemical diffusion coefficient of uranium dioxide. *J. Am. Ceram. Soc.* 53, 369–373. doi:10.1111/j.1151-2916.1970.tb12134.x

Lindemer, T. B., and Besmann, T. M. (1985). Chemical thermodynamic representation of $UO_{2\pm x}$. *J. Nucl. Mater.* 130, 473–488. doi:10.1016/0022-3115(85)90334-4

Maillard, S., Andersson, D., Freyss, M., and Bruneval, F. (2022). 'Assessment of atomistic data for predicting the phase diagram and defect thermodynamics. The example of non-stoichiometric uranium dioxide. *J. Nucl. Mater.* 569, 153864. doi:10.1016/j.jnucmat.2022.153864

Marin, J. F., and Contamin, P. (1969). Uranium and oxygen self-diffusion in UO2. *J. Nucl. Mater.* 30, 16–25. doi:10.1016/0022-3115(69)90164-0

Markin, T. L., and Bones, R. J. (1962a). The determination of changes in free energy for uranium oxides using a high temperature galvanic cell Part 1.

Markin, T. L., and Bones, R. J. (1962b). The determination of some thermodynamic properties of uranium oxides with O/U ratios between 2.00 and 2.03 using a high temperature galvanic cell Part 2.

Markin, T. L., Wheeler, V. J., and Bones, R. J. (1968). High temperature thermodynamic data for $UO_{2\pm x}$. *J. Inorg. Nucl. Chem.* 30, 807–817. doi:10.1016/0022-1902(68)80441-5

Matzke, H. (1987). Atomic transport properties in UO_2 and mixed oxides (U, Pu)O_2. *J. Chem. Soc. Faraday Trans.* 2, 1243. doi:10.1039/ft9908601243

Murch, G. E., Bradhurst, D. H., and De Bruin, H. J. (1975). Oxygen self-diffusion in non-stoichiometric uranium dioxide. *Philosophical Mag. A J. Theor. Exp. Appl. Phys.* 32, 1141–1150. doi:10.1080/14786437508228095

Murch, G. E., and Catlow, C. R. A. (1987). 'Oxygen diffusion in UO_2, ThO_2 and PuO_2 a review. *J. Chem. Society-Faraday Trans. Ii* 83, 1157–1169. doi:10.1039/f29878301157

Murch, G. E., and Thorn, R. J. (1978). 'The mechanism of oxygen diffusion in near stoichiometric uranium dioxide. *J. Nucl. Mater.* 71, 219–226. doi:10.1016/0022-3115(78)90419-1

Nerikar, P., Watanabe, T., Tulenko, J. S., Phillpot, S. R., and Sinnott, S. B. (2009). 'Energetics of intrinsic point defects in uranium dioxide from electronic-structure calculations. *J. Nucl. Mater.* 384, 61–69. doi:10.1016/j.jnucmat.2008.10.003

Petit, T., Lemaignan, C., Jollet, F., Bigot, B., and Pasturel, A. (1998). 'Point defects in uranium dioxide. *Philosophical Mag. B-Physics Condens. Matter Stat. Mech. Electron. Opt. Magnetic Prop.* 77, 779–786. doi:10.1080/014186398259176

Ruello, P., Chirlesan, G., Petot-Ervas, G., Petot, C., and Desgranges, L. (2004). 'Chemical diffusion in uranium dioxide – influence of defect interactions. *J. Nucl. Mater.* 325, 202–209. doi:10.1016/j.jnucmat.2003.12.007

Staicu, D., Wiss, T., Rondinella, V. V., Hiernaut, J. P., Konings, R. J. M., and Ronchi, C. (2010). 'Impact of auto-irradiation on the thermophysical properties of oxide nuclear reactor fuels. *J. Nucl. Mater.* 397, 8–18. doi:10.1016/j.jnucmat.2009.11.024

Terentyev, D. (2007). 'Molecular dynamics study of oxygen transport and thermal properties of mixed oxide fuels. *Comput. Mater. Sci.* 40, 319–326. doi:10.1016/j.commatsci.2007.01.002

Tetenbaum, M., and Hunt, P. D. (1968). 'High-Temperature thermodynamic properties of oxygen-deficient urania. *J. Chem. Phys.* 49, 4739–4744. doi:10.1063/1.1669953

Tiwary, P., van de Walle, A., and Gronbech-Jensen, N. (2009). '*ab initio* construction of interatomic potentials for uranium dioxide across all interatomic distances. *Phys. Rev. B* 80, 174302. doi:10.1103/physrevb.80.174302

Ugajin, M. (1983). 'Measurements of O/U ratio and oxygen potential for UO_{2+x} ($0 \leq x \leq 0.1$). *J. Nucl. Sci. Technol.* 20, 228–236. doi:10.1080/18811248.1983.9733384

Vathonne, E., Wiktor, J., Freyss, M., Jomard, G., and Bertolus, M. (2014). 'DFT + U investigation of charged point defects and clusters in UO2. *J. Phys. Condens Matter* 26, 325501. doi:10.1088/0953-8984/26/32/325501

Watanabe, M., Kato, M., and Sunaoshi, T. (2020). Oxygen self-diffusion in near stoichiometric (U, Pu)O2 at high temperatures of 1673-1873 K. *J. Nucl. Mater.* 542, 152472. doi:10.1016/j.jnucmat.2020.152472

Wheeler, V. J. (1971). High temperature thermodynamic data for UO2−x. *J. Nucl. Mater.* 39, 315–318. doi:10.1016/0022-3115(71)90151-6

Wheeler, V. J., and Jones, I. G. (1972). Thermodynamic and composition changes in $UO_{2\pm x}$ ($x < 0.005$) at 1950 K. *J. Nucl. Mater.* 42, 117–121. doi:10.1016/0022-3115(72)90018-9

Willis, B. T. M. (1987). 'Crystallographic studies of anion-excess uranium-oxides. *J. Chem. Society-Faraday Trans. Ii* 83, 1073–1081. doi:10.1039/f29878301073

Yu, J., Devanathan, R., and Weber, W. J. (2009). 'First-principles study of defects and phase transition in UO_2. *J. Phys. Condens Matter* 21, 435401. doi:10.1088/0953-8984/21/43/435401

Yun, Y. S., and Kim, W. W. (2007). "First principle studies on electronic and defect structures of UO_2, ThO_2, and PuO_2," in Proceedings of the KNS spring meeting. *Republic of Korea*, daejeon, South Korea, (KNS).